MEASUREMENT OF NON-LINEAR INSERT MAGNETS*

F. H. O'Shea†, R. Agustsson, A. Murokh, E. Spranza,
RadiaBeam Technologies, Santa Monica, CA 90404, USA
S. Nagaitsev, A Valishev, Fermilab, Batavia, IL 60510, USA

Abstract

Fermilab's Integrable Optics Test Accelerator (IOTA) is an electron storage ring designed for testing advanced accelerator physics concepts, including implementation of non-linear integrable beam optics and experiments on optical stochastic cooling. In this report we describe the contribution of RadiaBeam Technologies to the IOTA project which includes non-linear magnet engineering, prototype fabrication and measurement.

INTRODUCTION

IOTA is an electron ring designed as a proof-of-principle of non-linear integrable optics [1] at the ASTA facility [2]. Nonlinear optics are predicted to increase stability of the electron beam through Landau damping [3] and the natural tune spread of the electron beam will also increase dynamic aperture [1], leading to more intense beams in high-energy physics machines. The goal of the project is to study single particle dynamics in the non-linear regime using a 150 MeV electron beam in a ∼40 m circumference ring with 4 non-linear inserts that are each 2 m long [4]. While the beam dynamics of the non-linear optics system is being studied at Fermilab, the magnetic inserts are being designed and manufactured at RadiaBeam Technologies.

In this paper we discuss the magnetic design and tolerance requirements of the IOTA inserts and the measurement system being built to measure the first prototype of these unique magnets. The goals of the prototype magnet insert are to gain experience manufacturing a complex geometry, determine the cross-talk between adjacent magnet segments, and measure the field of a challenging insert that is tens of centimeters long with a sub-centimeter aperture.

DESIGN

The approach to this problem is the standard magnetostatic approach [5]: find the equipotential surfaces and choose one to fill with iron, correct the edge fields for the finite extent of the real magnets and then magnetize that iron via a current carrying coil on a "far off" yoke. The magnetostatic problem is defined in terms of the magnetic vector potential for a 2D object:

$$A_z(x,y,s) = \frac{B\rho\, c^2\, t}{\beta(s)} \sum_{n=1}^{\infty} \frac{2^{2n-1} n!(n-1)!}{(2n)!} \times \left(\frac{x^2+y^2}{\beta(s)\, c^2}\right)^n \cos\left[2n \arctan\left(\frac{y}{x}\right)\right]. \quad (1)$$

Where $B\rho$ is the magnetic rigidity of the particles, c is a scale factor with units $m^{1/2}$, t is a unitless strength parameter, x, y and s are the horizontal, vertical and longitudinal coordinates, respectively, and $\beta(s) = \beta^* + \frac{s^2}{\beta^*}$ is the beta-function in the non-linear insert with $\beta^* = 0.727$ m at the longitudinal center of the insert.

The vector potential (and as we will see, the scalar potential) is clearly continuous in the longitudinal coordinate but it would be very difficult to create a single 2 m long device that varies continuously to produce the desired scaling. Accordingly, the 2 m device is divided into 20 sections of constant parameters that are 6.5 cm long, between each section is a 3.5 cm long non-magnetic block (or air gap) used to separate the different segments. Because of the symmetry around the longitudinal center of the device, there are 10 different segments. The segments are labeled 1 through 10 with 1 being nearest the center of the 2 m device and 10

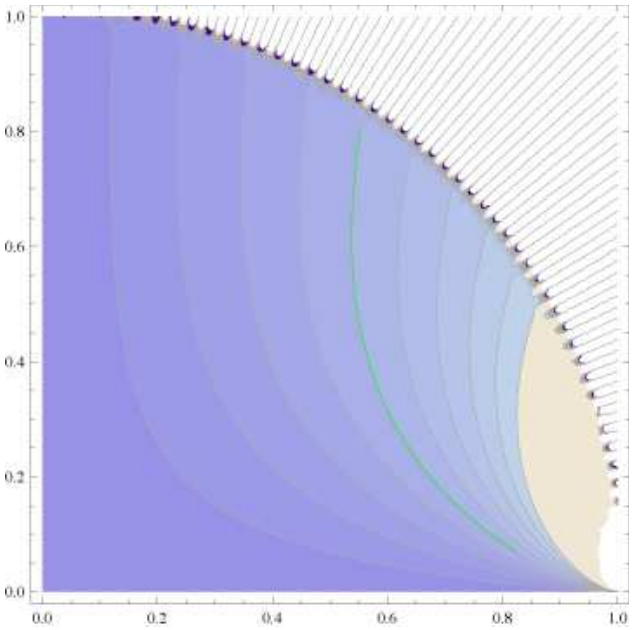

Figure 1: Contour plot of the equipotential lines of $\phi(x_N, y_N)$. The superimposed green line is the line taken for the face of the poles.

* Work supported by DOE under contract DE-SC0009531.
† oshea@radiabeam.com

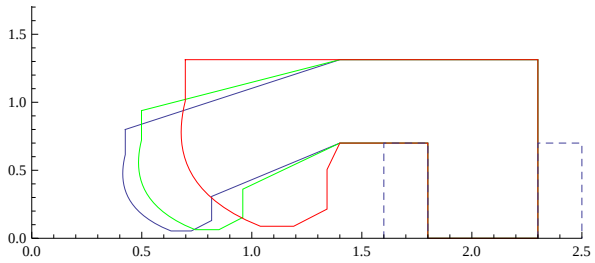

Figure 2: Real space outline of the 2D IOTA design for segments 1 (blue), 5 (green) and 10 (red), including a continuous return yoke. The dashed lines show the outline of the excitation coils. All dimensions are in centimeters.

being the outer most segment.

To lowest order, the problem is limited to a 2D plane, so the scalar potential is related to the vector potential via a $\pi/2$ rotation about the longitudinal axis [6]:

$$\phi(x_N, y_N) = t \sum_{n=1}^{\infty} \frac{2^{2n-1} n!(n-1)!}{(2n)!} \times \left(\frac{x_N^2 + y_N^2}{c^2} \right)^n \sin\left[2n \arctan\left(\frac{y_N}{x_N}\right)\right]. \quad (2)$$

Here, the scalar potential has been normalized such that $\Phi(x, y, s) \equiv \frac{B\rho c^2}{\beta(s)} \phi(x/\beta^{1/2}, y/\beta^{1/2})$ with $x_N \equiv x/\beta^{1/2}$ and $y_N \equiv y/\beta^{1/2}$. Because we know the scaled form of the potential and how the beta-function evolves through the non-linear magnet, we can solve for the pole face once and then scale it via the beta-function for all of the magnets. Further, because of the four-fold symmetry of the problem, we need only find the solution in one quadrant. The equipotential lines of the scalar potential in Eq. 2 are shown in Fig. 1. The green line in Fig. 1 shows the contour that will be used to define the pole faces. Because the solution is scaled by $\beta(s)$, this is the face for all of the magnets.

We note here that the potentials given by Eqs. 1 and 2 have singularities at ($x_N = \pm c$, $y_N = 0$), so whatever solution is found can never include normalized coordinates greater than c. Further, because the singularities are located on the $y = 0$ line, the vertical aperture is larger than the horizontal aperture.

In order to make the design easier to produce we have decided to make a single yoke design for all of the different pole tips. This way, the yokes can be produced en masse while the tighter tolerance pole tips are made for each of the segments separately. Fig. 2 shows a 2D outline of poles 1 (the smallest pole, it is the pole closest to the longitudinal symmetry point), 5 and 10 (the largest pole) of the IOTA insert design along with a continuous return yoke and a single excitation coil. The curved surface of each segment is given by the green line in Fig. 1.

Above the curved pole tip, a straight face is extended to 1.3 times the height of the highest point on the curved face. This straight corner improves the agreement between the simulation results and the desired field. The value was found via 2D optimization of the field using the code Poisson [7]. The height of the yoke is defined by the height of the pole face extension for the number 10 segment. On the lower side, the curved face is cut off by a flat section that is "chamfered" on the outside edge (to the right in Fig. 2) to prevent field concentration there. These underside changes are made in the scaled coordinate system, so they are different for each magnet.

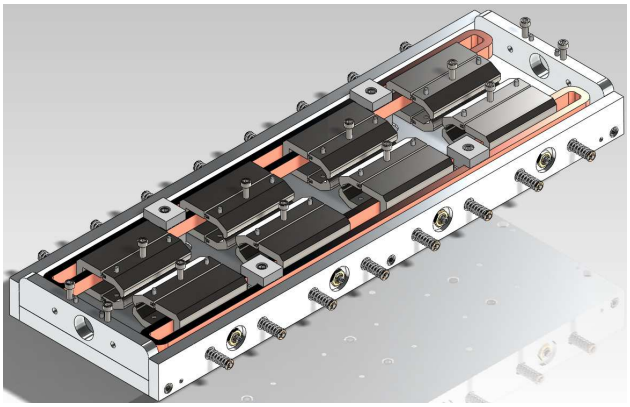

Figure 3: Isometric view of the IOTA insert prototype. A plate on top has been hidden to show detail below. The copper items are the excitation coils, the dark grey items are the steel poles and return yokes and light grey items are aluminum.

An isometric view of the prototype insert can be seen in Fig. 3. The prototype insert will contain 4 complete segments. Because the smallest aperture comes from the number 1 pole, the prototype insert will have the following segments (in order): 1, 1, 2, 3. This combination of segments allows us to measure the smallest aperture magnets and the coupling between segments. 3D simulation using the code Maxwell [8] has shown that the longitudinal symmetry point of a full length insert will be faithfully reproduced between the two number 1 poles in the prototype.

NONLINEAR MAGNET REQUIREMENTS

Figure 4: Close up image of the tongue and groove reluctance gap.

The magnets shown in Fig. 2 are closed yoke magnets. However, because the beta-function of the electron beam evolves along the length of the insert, each of the 10 segments requires a different excitation magnitude. To reduce the number of power supplies needed, we have decided to

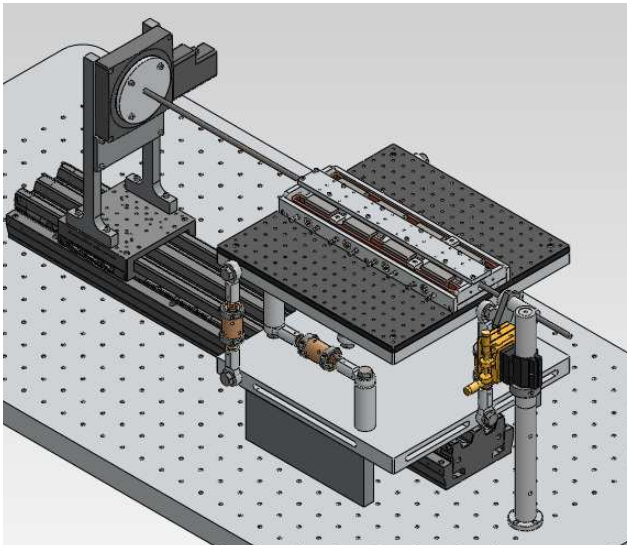

Figure 5: View of the IOTA insert measurement system.

use a single excitation coil for all of the yokes and to tune the field in each segment using a reluctance gap that can be set by moving the return yoke of each segment individually. If the reluctance gap were comprised of two flat faces, the required precision of the position of the yoke relative to a fixed pole tip is very tight, a few micrometers. To reduce the required tolerance we opted for a tongue and groove approach, this results in a required positional tolerance of $\sim$50 μm. A close up of the tongue and groove reluctance gap can be seen in Fig. 4.

The field quality requirements were defined using a frequency map analysis [4], the analysis indicates that a good field region of $|y| \approx c$ and $|x| \approx c/2$, with good being defined as difference from the ideal field by less than 1%, is required. Further, the magnetic center of the segments must be placed along the same line with an accuracy of 50 μm or less. To compare the magnetostatic simulations to the theoretical field, the simulated field is compared to the ideal field on the y-axis (B_x) and x-axis (B_y). Of the above defined magnets, the number 1 pole has the worst field quality: the difference is less than 0.5% at all points within ($x < 0.6c$,$y < 0.8c$). Therefore, simulations show that all magnets are potentially within the desired tolerance. Harmonic analysis of the fields produced by Poisson shows that the field faithfully reproduces the quadrupole and octopole moments with 0.1% of the desired values while the dodecapole moment is within 3% of the desired value (r_N = 0.5). The fields in the aperture are quite small at $B \leq$ 100 G, using t=0.45, c = 0.009 m$^{1/2}$ and $B\rho$ = 0.502 T-m, which are the design parameters for the prototype.

MEASUREMENT SYSTEM

To measure the magnetic field of the prototype insert requires that we design a measurement system with over 40 cm of travel in the longitudinal direction that can fit within circular gap of $\sim$10 mm diameter within the number 1 pole

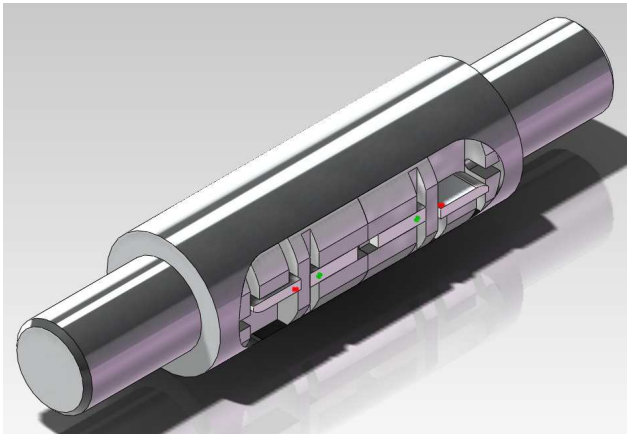

Figure 6: View of the hall probe holder showing the custom mechanics to allow probe motion in the radial direction. The red and green crosses are the locations of the hall probes.

(see Fig. 5). Additionally, the hall probe must be able to move within this 10 mm diameter gap. To accomplish this, we have designed a "rod and radius" system wherein a set of miniature hall probes [9] are mounted in a custom holder in a rod of the specified diameter (see Fig. 6). The rod is moved longitudinally via a linear motion stage and rotationally via a rotational stage. The radius is set manually with a set screw. This design will allow us to measure a large fraction of the desired aperture. We will use 4 hall probes that are separated longitudinally in the probe holder, such that two different radii within the IOTA insert aperture can be measured in a single, automated longitudinal scan (see Fig. 6). We intend to zero and measure each of the probes in a pair of common standards and to have an overlap region that can be measured by both sets of probes for direct comparison. At the time of publication, the IOTA insert is being manufactured and the measurement design is being completed.

REFERENCES

[1] V. Danilov and S. Nagaitsev, Phys. Rev. ST Accel. Beams 13, 084002 (2010).

[2] J. Leibfritz et al., IPAC'12, New Orleans, USA, May 2012, MOOAC02, p. 58, http://www.JACoW.org

[3] S. Nagaitsev, A. Valishev and V. Danilov, HB2010, Morschach, Switzerland, Sept. 2010, THO1D01, p. 676, http://epaper.kek.jp/HB2010/

[4] A. Valishev, et al., IPAC'12, New Orleans, USA, May 2012, TUPPC090, p. 1371, http://www.JACoW.org

[5] H. Wiedemann, *Particle Accelerator Physics, vol. I, 2nd Ed.*, (Berlin: Springer, 2003), 97.

[6] K. Halbach, Nucl. Instr. Meth. A 169, 1 (1980).

[7] K. Halbach and R. F. Holsinger, Particle Accel. 7, 213 (1976).

[8] http://www.ansys.com

[9] Arepoc s.r.o., http://www.arepok.sk